

Computing complex and real tropical curves using monodromy

Daniel A. Brake^{*} Jonathan D. Hauenstein[†] Cynthia Vinzant[‡]

March 1, 2022

Abstract

Tropical varieties capture combinatorial information about how coordinates of points in a classical variety approach zero or infinity. We present algorithms for computing the rays of a complex and real tropical curve defined by polynomials with constant coefficients. These algorithms rely on homotopy continuation, monodromy loops, and Cauchy integrals. Several examples are presented which are computed using an implementation that builds on the numerical algebraic geometry software **Bertini**.

Introduction

Tropical geometry is a field of mathematics that uses combinatorial structures to study problems in algebraic geometry. It has proven to be a powerful tool for understanding real and complex varieties. Computations with tropical varieties can extract delicate combinatorial properties of algebraic varieties, and tropical methods can be used to construct finely-tuned examples of varieties with desired properties, e.g., [2, 30].

Most of the current algorithms for computing tropical varieties are symbolic and are restricted to tropical varieties defined over algebraically-closed fields. The past few years have seen the development of new techniques based on numerical algebraic geometry for computing complex tropical varieties in the case of hypersurfaces [16] and curves [20]. In this paper, we present a new algorithm for computing complex tropical curves, which we then enhance to compute real tropical curves. We have implemented these algorithms using a combination of Matlab and **Bertini** [7] available at [10].

We anticipate that the numerical computation of tropical curves represents a first step towards the numerical computations of higher-dimensional tropical varieties. Another reason to focus on curves, as mentioned in [20], is that the computation of tropical curves is an

^{*}Department of Applied and Computational Mathematics and Statistics, University of Notre Dame, Notre Dame, IN 46556 (dbrake@nd.edu, danielthebrake.org).

[†]Department of Applied and Computational Mathematics and Statistics, University of Notre Dame, Notre Dame, IN 46556 (hauenstein@nd.edu, www.nd.edu/~jhauenst).

[‡]Department of Mathematics, North Carolina State University, Raleigh, NC 27695 (clvinzan@ncsu.edu, www.math.ncsu.edu/~clvinzan).

internal step in the computation of other tropical varieties. Moreover, to the best of our knowledge, no other computational techniques exist for real tropical curves. We hope to extend this to higher-dimensional real tropical varieties as well.

The remainder of the paper is organized as follows. In the first section, we summarize the necessary background and notation for tropical varieties. Cauchy's integral formula and projectivization are discussed in Section 2. In Section 3, we present our algorithms for computing complex and real tropical curves and prove their correctness. Implementation of these algorithms is discussed in Section 4. Finally, we conclude in Section 5 with examples.

1 Background on tropical geometry

Let \mathbb{k} be a field and I be an ideal in the polynomial ring $\mathbb{k}[x_1, \dots, x_n]$. For any subset S of the field \mathbb{k} , we denote $\mathcal{V}_S(I)$ as zero set in S^n of the polynomials in I . The most often cases are $S = \mathbb{k}$ and the set of non-zero elements $S = \mathbb{k}^*$.

The set of Puiseux series over a field \mathbb{k} , denoted $\mathbb{k}\{\{t\}\}$, is the union over all positive integers n of the formal Laurent series in $t^{1/n}$, namely

$$\mathbb{k}\{\{t\}\} = \bigcup_{n \geq 1} \mathbb{k}((t^{1/n})) = \bigcup_{n \geq 1} \left\{ \sum_{j=k}^{\infty} c_j t^{j/n} \mid k \in \mathbb{Z}, c_j \in \mathbb{k} \right\}. \quad (1)$$

The field $\mathbb{C}\{\{t\}\}$ is algebraically closed and $\mathbb{R}\{\{t\}\}$ is real closed. The field of Puiseux series has a valuation, $\text{val} : \mathbb{k}\{\{t\}\}^* \rightarrow \mathbb{Q}$, and coefficient map, $\text{coeff} : \mathbb{k}\{\{t\}\}^* \rightarrow \mathbb{k}^*$, given by

$$\text{val} \left(\sum_q c_q t^q \right) = \min\{q \mid c_q \neq 0\} \quad \text{and} \quad \text{coeff}(y) = c_{\text{val}(y)}.$$

If a Puiseux series y converges for t in a neighborhood of zero then $\text{coeff}(y)t^{\text{val}(y)}$ gives its order of growth around $t = 0$. Both maps $\text{val}(\cdot)$ and $\text{coeff}(\cdot)$ extend to $\mathbb{k}\{\{t\}\}^n$ coordinate-wise.

Given an ideal $I \subset \mathbb{k}[x_1, \dots, x_n]$, consider the zeros of the polynomials in I over $\mathbb{k}\{\{t\}\}^n$ and their valuations in \mathbb{Q}^n . For technical reasons, we actually consider the negative of the valuation map, corresponding to the “max” convention. Letting this run over all solutions and taking the Euclidean closure in \mathbb{R}^n yields the *tropical variety* over \mathbb{k} of the ideal I .

Definition 1. Given an ideal $I \subset \mathbb{k}[x_1, \dots, x_n]$, the **tropical variety over \mathbb{k}** , denoted $\text{Trop}_{\mathbb{k}}(I) \subset \mathbb{R}^n$, is the closure of the image of its variety over $\mathbb{k}\{\{t\}\}^*$ under the negative valuation map,

$$\text{Trop}_{\mathbb{k}}(I) = -\overline{\text{val}(\mathcal{V}_{\mathbb{k}\{\{t\}\}^*}(I))}.$$

We call $\text{Trop}_{\mathbb{C}}(I)$ the **tropical variety** of I and $\text{Trop}_{\mathbb{R}}(I)$ the **real tropical variety** of I . As $\text{Trop}_{\mathbb{k}}(I)$ only depends on the variety $\mathcal{V}_{\mathbb{k}^*}(I)$, we will also use the notation $\text{Trop}_{\mathbb{k}}(\mathcal{V}(I))$.

In this paper, we will be particularly interested in locally convergent Puiseux series. For $\mathbb{k} = \mathbb{R}, \mathbb{C}$, replacing $\mathbb{k}\{\{t\}\}$ with locally convergent Puiseux series $\mathbb{k}\{\{t\}\}_{\text{conv}}$ does not change the image of a variety under the valuation map. That is, $\text{Trop}_{\mathbb{k}}(I) = -\overline{\text{val}(\mathcal{V}_{\mathbb{k}\{\{t\}\}_{\text{conv}}}(I))}$.

The tropical variety $\text{Trop}_{\mathbb{C}}(I)$ is closely related to the initial ideals of the ideal I as follows. For $\alpha \in \mathbb{N}^n$, let x^α denote $x_1^{\alpha_1} x_2^{\alpha_2} \cdots x_n^{\alpha_n}$. Given $w \in \mathbb{R}^n$ and a polynomial $f(x) = \sum_{\alpha} f_{\alpha} x^{\alpha}$,

the initial form of f with respect to w , denoted $\text{in}_w(f)$, is the sum of the terms $f_\alpha x^\alpha$ which maximize $w \cdot \alpha$. For an ideal $I \subset \mathbb{C}[x_1, \dots, x_n]$, the initial ideal of I with respect to w , denoted $\text{in}_w(I)$, is the ideal generated by the initial forms of elements of I , namely

$$\text{in}_w(I) = \langle \text{in}_w(f) \mid f \in I \rangle.$$

Suppose $y \in \mathbb{k}\{\{t\}\}^n$ is an n -tuple of non-zero Puiseux series with valuation $\text{val}(y) \in \mathbb{Q}^n$ and leading coefficients $\text{coeff}(y) \in (\mathbb{k}^*)^n$. If y lies in the variety $\mathcal{V}_{\mathbb{k}\{\{t\}\}}(I)$ for some ideal $I \subset \mathbb{k}[x_1, \dots, x_n]$, then $w = -\text{val}(y)$ belongs to the tropical variety $\text{Trop}_{\mathbb{k}}(I)$, and $\text{coeff}(y)$ belongs to the variety of the initial ideal $\mathcal{V}_{\mathbb{k}}(\text{in}_w(I))$. In particular, $\mathcal{V}_{\mathbb{k}}(\text{in}_w(I)) \cap (\mathbb{k}^*)^n$ is non-empty which implies that $\text{in}_w(I)$ cannot contain a monomial. Over \mathbb{C} , the converse holds and is known as the fundamental theorem of tropical geometry. Indeed, for $\mathbb{k} = \mathbb{C}$, tropical varieties have very specific combinatorial structure, which we summarize from [21, Theorems 3.2.3 and 3.3.8]:

Theorem 2. *Let $I \subset \mathbb{C}[x_1, \dots, x_n]$ be a prime ideal that defines a d -dimensional variety $\mathcal{V}_{\mathbb{C}^*}(I)$. Then, the tropical variety $\text{Trop}_{\mathbb{C}}(I)$ is the support of a pure d -dimensional rational polyhedral fan. It is the set of weights for which the initial ideal of I contains no monomials: $\text{Trop}_{\mathbb{C}}(I) = \{w \in \mathbb{R}^n \mid \text{in}_w(I) \text{ does not contain a monomial}\}$.*

Remark 3. One can associate a multiplicity to each maximal cone in the tropical variety $\text{Trop}_{\mathbb{C}}(I)$. Each irreducible component of the variety $\mathcal{V}_{\mathbb{C}^*}(\text{in}_w(I))$ contributes to the multiplicity of the ray w by the multiplicity of the corresponding minimal prime in $\text{in}_w(I)$. See [21, §3.4] for details. With multiplicities, the tropical complex variety is *balanced*. In particular, if the tropical variety is a union of rays $\vec{r}_1, \dots, \vec{r}_s$ with multiplicities m_1, \dots, m_s , and r_i is the primitive integer point on the ray \vec{r}_i , the weighted sum $m_1 r_1 + \dots + m_s r_s \in \mathbb{R}^n$ is zero.

As in classical algebraic geometry, real varieties provide subtle challenges for tropicalization. There are some similarities to the complex case. In particular, Alessandrini [1] recently showed that $\text{Trop}_{\mathbb{R}}(I)$ is a rational polyhedral fan related to the real variety $\mathcal{V}_{\mathbb{R}^*}(I)$.

Theorem 4 ([1]). *For an ideal $I \in \mathbb{R}[x_1, \dots, x_n]$, the real tropical variety $\text{Trop}_{\mathbb{R}}(I)$ is a rational polyhedral fan in \mathbb{R}^n whose dimension is at most the dimension of the variety $\mathcal{V}_{\mathbb{R}^*}(I)$.*

In general, we only know that $\text{Trop}_{\mathbb{R}}(I) \subseteq \text{Trop}_{\mathbb{C}}(I)$. In fact, $\text{Trop}_{\mathbb{R}}(I)$ is not necessarily a subfan of the Gröbner fan of I . For examples, see [1, Fig. 7] or [28, Section 2]. The real tropical variety $\text{Trop}_{\mathbb{R}}(I)$ need not have the same dimension as $\mathcal{V}_{\mathbb{R}}(I)$, it need not satisfy any balancing conditions, and it may not be pure of any dimension.

Example 5. Consider the sextic polynomial $f = x^6 - x^3 + y^2$. The complex tropical variety $\text{Trop}_{\mathbb{C}}(f)$ consists of the rays spanned by $(-2, -3)$, $(1, 3)$, and $(0, -1)$, with multiplicities 1, 2, and 3, respectively, as shown in Figure 1. In this case, we can use power series expansions to explicitly find solutions to $f = 0$ over $\mathbb{C}\{\{t\}\}$ with these valuations, e.g.:

$$\begin{aligned} (x, y) &= \left(t^2, t^3 - \frac{t^9}{2} - \frac{t^{15}}{8} - \frac{t^{21}}{16} + \dots \right) & \rightarrow & -\text{val}(x, y) = (-2, -3) \\ (x, y) &= \left(\frac{1}{t}, -\frac{i}{t^3} + \frac{i}{2} + \frac{it^3}{8} + \frac{it^6}{16} + \dots \right) & \rightarrow & -\text{val}(x, y) = (1, 3) \\ (x, y) &= \left(1 - \frac{t^2}{3} - \frac{4t^4}{9} - \frac{77t^6}{81} + \dots, t \right) & \rightarrow & -\text{val}(x, y) = (0, -1). \end{aligned}$$

Here, the Puiseux series $x, y \in \mathbb{C}\{\{t\}\}$ are locally convergent near $t = 0$ meaning that these tuples locally parametrize a path in $\mathcal{V}_{\mathbb{C}^*}(I)$. The first and last actually belong to $\mathbb{R}\{\{t\}\}$, and therefore contribute to rays in $\text{Trop}_{\mathbb{R}}(f)$. On the other hand, since the real variety $\mathcal{V}_{\mathbb{R}}(f)$ is compact, there is no point in $\mathcal{V}_{\mathbb{R}\{\{t\}\}}(f)$ with valuation $(-1, -3)$.

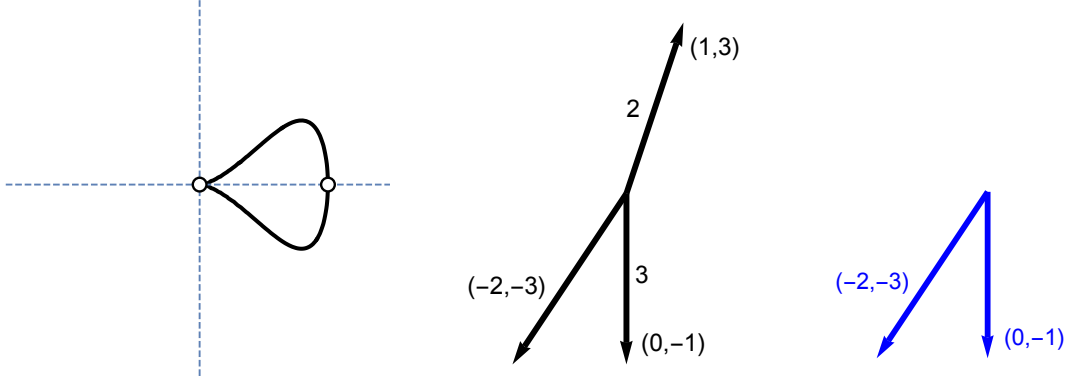


Figure 1: The real points of a sextic plane curve, its complex tropical variety with multiplicities listed when > 1 , and its real tropical variety.

Remark 6. In this paper, we avoid assigning multiplicities to rays in the real tropical variety, as it is not clear to us what the correct notion of multiplicity should be in this case. As the example below shows, it is not enough to count the multiplicity of real minimal primes associated to the initial ideal of a ray. However, in the process of computing a real tropical curve, one can compute the number of real Puiseux series with a given valuation w that define different germs of a function around a point $p \in \mathcal{V}_{\mathbb{R}^*}(\text{in}_w(I))$, which may provide some notion of multiplicity in this case.

Example 7. Consider the polynomial $f = ((x - 1)^2 + y^2) \cdot ((x - 1)^2 - y^2)$. Its variety is the union of four lines, one real pair and one complex conjugate pair. The ray spanned by the vector $w = (0, -1)$ lies in both the real and complex tropical variety. The corresponding initial form is $\text{in}_w(f) = (x - 1)^4$ so this ray has multiplicity four in $\text{Trop}_{\mathbb{C}}(f)$. Even though all four roots of $\text{in}_w(f)$ are real, the contribution to the multiplicity from the real points is only two, with the other contribution of two to the multiplicity arising from nonreal points. An irreducible polynomial with the same local behavior is $f + y^6$.

Remark 8. The real part of the complex torus $(\mathbb{C}^*)^n$ naturally breaks up into orthants with a given sign pattern. Paths in $(\mathbb{R}^*)^n$ approaching 0 or ∞ do so from within some orthant. In order to keep track of this data, consider the *signed valuation map*

$$\text{sval} : \mathbb{R}\{\{t\}\}^* \rightarrow \mathbb{Q} \times \{+, -\} \quad \text{given by} \quad \text{sval}(x) = \begin{cases} (\text{val}(x), +) & \text{if } \text{coeff}(x) > 0 \\ (\text{val}(x), -) & \text{if } \text{coeff}(x) < 0, \end{cases}$$

as in [3, 22, 26, 30]. The map sval extends coordinate-wise to $(\mathbb{R}\{\{t\}\}^*)^n$. For an ideal $I \subset \mathbb{R}[x_1, \dots, x_n]$, the **signed real tropical variety** $\text{sTrop}_{\mathbb{R}}(I)$ is the image of the variety $\mathcal{V}_{\mathbb{R}\{\{t\}\}^*}(I)$ under the map $-\text{sval}$, where the negation acts on the vector in \mathbb{Q}^n and fixes

the sign pattern in $\{\pm\}^n$. The signed tropical variety lies in the disjoint union of 2^n copies of \mathbb{Q}^n . The **positive tropical variety** $\text{Trop}_+(I)$ is the part of the signed tropical variety lying in the positive copy, $\mathbb{Q}^n \times (+, \dots, +)$, and has appeared in [4, 25], among others.

Example 9. Consider the quartic polynomial $f = x^4 + y^4 - (x - y)^2(x + y)$. The real tropical variety $\text{Trop}_{\mathbb{R}}(f)$ consists of the rays spanned by the vectors $(0, -1)$, $(-1, 0)$, and $(-1, -1)$. For example, the Puiseux series $(x, y) = (1 - t - 2t^2 + \dots, t)$ lies the variety of f . Its image under $-\text{sval}$ is $((0, -1), (+, +))$. Replacing t with $-t$ gives a point in $\mathbb{R}\{\{t\}\}^2$ in the variety of f with $-\text{sval}(x, y) = ((0, -1), (+, -))$. The real variety of f along with its signed tropical variety is shown in Figure 2. We will return to this in Example 18.

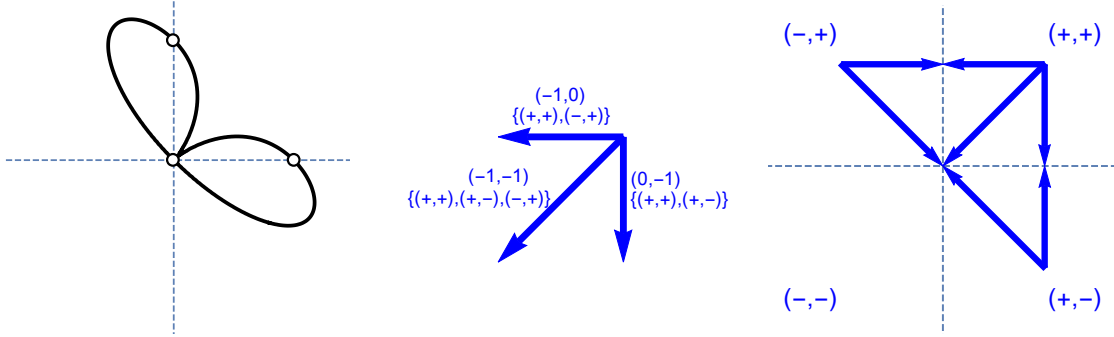


Figure 2: The real points of a quartic plane curve with its signed tropical variety.

2 Cauchy's integral formula and projectivization

2.1 Monodromy and Cauchy's integral formula

Monodromy is related to Riemann surfaces, branch cuts, and singularities in that one aims to study an object by walking around in closed loops which can induce a non-trivial action. In the context of tropical curves, we will always reduce down to the locally analytic case by performing a local uniformization of complex curves, e.g., [24, Thm. A.3.2], after computing the *cycle number*, which we now define for the case of interest. Let $C \subset \mathbb{C}^n$ be a curve not contained in a hyperplane and $p \in C$ whose j^{th} coordinate $p_j = \tau \neq 0$ is sufficiently small. This setup defines $P(s) \in C$ where $P(1) = p$ and $P_j(s) = \tau s$, which is smooth for $0 < |s| \leq 1$. For $\theta \geq 0$, consider the continuous and periodic function $\theta \mapsto P(e^{2\pi i \theta})$. The **cycle number** for the path $P(s)$ is the minimum positive integer c such that $P(e^{2\pi i c}) = p = P(1)$. Since $C \cap \mathcal{V}(x_j - \tau)$ consists of at most $\deg C$ points, it immediately follows that $1 \leq c \leq \deg C$.

In terms of Puiseux series, the cycle number c is the minimum positive integer n such that every coordinate of $P(s)$ lies in $\mathbb{C}((s^{1/n}))$. That is, the cycle number c is the minimum positive integer n such that the function $s \mapsto P(s^n)$ is analytic on $0 < |s| \leq 1$. In particular, if $\lim_{s \rightarrow 0} P(s) \in \mathbb{C}^n$, then each coordinate of the function $s \mapsto P(s^c)$ is analytic on $|s| \leq 1$.

Suppose a function $f : \mathbb{C} \rightarrow \mathbb{C}$ is analytic on the unit disk in \mathbb{C} , specifically on and inside the closed loop γ given by $\{e^{i\theta} \mid 0 \leq \theta \leq 2\pi\}$. For $k \in \mathbb{Z}_{\geq 0}$, Cauchy's integral formula yields

$$\frac{f^{(k)}(0)}{k!} = \frac{1}{2\pi i} \int_{\gamma} \frac{f(z)}{z^{k+1}} dz = \frac{1}{2\pi} \int_0^{2\pi} \frac{f(e^{i\theta})}{(e^{i\theta})^k} d\theta. \quad (2)$$

In particular, f has a power series expansion around $z = 0$ and its valuation is the smallest k for which $f^{(k)}(0)$ is non-zero. Using numerical path tracking, one can generate a discretization of γ and numerically approximate $f^{(k)}(0)$.

2.2 Projectivization and affine patches

In addition to reducing down to the locally analytic case, another key idea in our algorithm is to work on an affine patch for which the valuation of each point of interest is nonnegative. This corresponds with finite length solution paths that limit to a coordinate hyperplane. These paths can be parametrized by tuples of Puiseux series with nonnegative valuations and therefore correspond to points in the tropical variety with nonpositive coordinates.

To that end, suppose that $C \subset (\mathbb{C}^*)^n$ is a curve defined by an ideal $I \subset \mathbb{C}[x_1, \dots, x_n]$. In order to simplify the computations, we will first consider the closure of C in \mathbb{P}^n , namely

$$\overline{C} = \overline{\{[1 : y_1 : \dots : y_n] \mid (y_1, \dots, y_n) \in C\}} \subset \mathbb{P}^n.$$

The finitely many points in the boundary $\partial C = \overline{C} \setminus C$ are contained in the coordinate hyperplanes in \mathbb{P}^n . The “hyperplane at infinity” in $(\mathbb{C}^*)^n$ becomes one of these coordinate hyperplanes, namely $\{x_0 = 0\}$.

We next restrict to an affine coordinate patch. That is, for a nonzero vector $v \in \mathbb{C}^{n+1}$, consider the intersection \widehat{C} of the affine cone over \overline{C} with the plane defined by $v \cdot x = 1$. Since the set of points of interest on \overline{C} are its intersections with the coordinate hyperplanes, we require that each of these finitely-many points correspond to a finite point in the coordinate patch defined by $v \cdot x = 1$, i.e.,

$$\{x \in \mathbb{P}^n \mid v \cdot x = 0\} \cap \{x \in \overline{C} \mid \text{some coordinate } x_i \text{ is zero}\} = \emptyset. \quad (3)$$

If $d = \deg C$, there are at most $(n+1)d$ points in the intersection of \overline{C} with the union of the coordinate hyperplanes. Hence, we must select $v \in \mathbb{C}^{n+1}$ outside of a hypersurface of degree at most $(n+1)d$. In practice, we select the vector $v \in \mathbb{C}^{n+1}$ randomly. When computing $\text{Trop}_{\mathbb{R}}$, the entries of the vector v should be real to maintain a relationship between the real points of C and the real points of \widehat{C} . Under these hypotheses, the complex and real tropical varieties of C can be recovered from those of \widehat{C} .

Proposition 10. *If $v \in (\mathbb{k}^*)^{n+1}$ satisfies (3) where $\mathbb{k} = \mathbb{R}$ or \mathbb{C} , then $\text{Trop}_{\mathbb{k}}(C)$ equals the image of $\text{Trop}_{\mathbb{k}}(\widehat{C}) \cap (\mathbb{R}_{\leq 0})^{n+1}$ under the map $(w_0, \dots, w_n) \mapsto (w_1 - w_0, \dots, w_n - w_0)$. Furthermore, for $\mathbb{k} = \mathbb{C}$, this map preserves multiplicities of rays from $\text{Trop}_{\mathbb{C}}(\widehat{C})$ to $\text{Trop}_{\mathbb{C}}(C)$.*

For the proof of this proposition below, we need two consequences of condition (3).

Lemma 11. *Let $\ell = v \cdot x \in \mathbb{C}[x_0, \dots, x_n]_1$ where $v \in (\mathbb{C}^*)^{n+1}$ satisfies (3), and suppose that $w \in \text{Trop}(\overline{C}) \cap (\mathbb{R}_{\leq 0})^{n+1}$ with $w_j = 0$ for some j and $w_k \neq 0$ for some k . Then the initial form $\text{in}_w(\ell)$ does not vanish at any point $a \in (\mathbb{C}^*)^{n+1}$ in the variety of the initial ideal $\text{in}_w(I(\overline{C}))$. In particular, $\text{in}_w(\ell)$ is not a zero-divisor modulo the ideal $\text{in}_w(I(\overline{C})) \subset \mathbb{C}[x_0^{\pm 1}, \dots, x_n^{\pm 1}]$.*

Proof. Let J denote the homogeneous ideal $I(\overline{C})$, and suppose that $\text{in}_w(\ell)$ vanishes at some point $a = (a_0, \dots, a_n) \in \mathcal{V}(\text{in}_w(J)) \cap (\mathbb{C}^*)^{n+1}$. Since each coordinate of w is non-positive and

some coordinate is zero, the initial form of ℓ is the sum $\sum_{i \in \mathcal{A}} v_i x_i$ where $\mathcal{A} = \{i \mid w_i = 0\}$. Taking e_i to be the i th coordinate vector, we see that $\ell(\sum_{i \in \mathcal{A}} a_i e_i) = \text{in}_w(\ell)(a) = 0$.

On the other hand, by [21, Prop. 3.2.11], there exists a point $y \in \mathcal{V}_{\mathbb{C}\{\{t\}\}^{\text{conv}}}(J)$ with $-\text{val}(y) = w$ and $\text{coeff}(y) = a$. The leading terms of y are then $(a_0 t^{-w_0}, \dots, a_n t^{-w_n})$, and the Puiseux series $y_i(t)$ converges for small enough t . Since each exponent $-w_i$ is nonnegative, the coordinates $y_i(t)$ converge for $t = 0$. Thus $y(0) = \sum_{i \in \mathcal{A}} a_i e_i$ belongs to \overline{C} .

Consider the point $p = \sum_{i \in \mathcal{A}} a_i e_i$. Since $w_j = 0$ and $w_k \neq 0$, the point p has j^{th} coordinate $a_j \neq 0$ and k^{th} coordinate zero. Also $\ell(p) = 0$ and $p \in \overline{C}$. Thus p belongs to the intersection in (3) and v does not satisfy condition (3). \square

Lemma 12. *Suppose that $J \subset \mathbb{C}[x_0, \dots, x_n]$ is homogeneous ideal, $\ell \in \mathbb{C}[x_0, \dots, x_n]_1$, and $w \in \mathbb{R}^{n+1}$. If $\text{in}_w(\ell)$ is not a zero-divisor modulo $\text{in}_w(J)$, then*

$$\text{in}_w(J + \langle \ell - 1 \rangle) = \text{in}_w(J) + \text{in}_w(\langle \ell - 1 \rangle). \quad (4)$$

Proof. The containment \supseteq is clear. To show the other containment, consider the set

$$S = \{(g, h) \mid \text{in}_w(g + (\ell - 1)h) \notin \text{in}_w(J) + \text{in}_w(\langle \ell - 1 \rangle)\} \subset J \times \mathbb{C}[x_0, \dots, x_n].$$

For the sake of contradiction, suppose that S is non-empty and take $(g, h) \in S$ with minimal $\deg(h)$. Since $\text{in}_w(g + (\ell - 1)h)$ is not equal to $\text{in}_w(g) + \text{in}_w((\ell - 1)h)$, the sum of these leading terms must be zero. Taking further initial forms with respect to $\mathbf{1} = (1, \dots, 1)$ yields $-\text{in}_1(\text{in}_w(g)) = \text{in}_1(\text{in}_w((\ell - 1)h)) = \text{in}_1(\text{in}_w(\ell - 1)) \cdot \text{in}_1(\text{in}_w(h))$.

If $\text{in}_w(\ell - 1) = 1$, then the ideals on both sides of (4) are the ideal $\langle 1 \rangle$ and thus equal. Therefore we may assume that $\text{in}_w(\ell) \neq 1$, in which case $\text{in}_1(\text{in}_w(\ell - 1)) = \text{in}_w(\ell)$. Putting this together with the arguments above, we see that the product $\text{in}_w(\ell) \cdot \text{in}_1(\text{in}_w(h))$ belongs to $\text{in}_1(\text{in}_w(J))$. Because J is homogeneous, the ideal $\text{in}_w(J)$ is also homogeneous, by [21, Lemma 2.4.2]. Hence $\text{in}_1(\text{in}_w(J)) = \text{in}_w(J)$. Thus, $\text{in}_w(\ell) \cdot \text{in}_1(\text{in}_w(h))$ belongs to the ideal $\text{in}_w(J)$. By assumption, $\text{in}_w(\ell)$ is not a zero-divisor modulo $\text{in}_w(J)$, so $\text{in}_1(\text{in}_w(h))$ must belong to $\text{in}_w(J)$. Therefore we can take $f \in J$ with $\text{in}_w(f) = \text{in}_1(\text{in}_w(h))$.

Now consider $(g', h') = (g + (\ell - 1)f, h - f)$. Since $f \in J$, $g + (\ell - 1)f$ belongs to J . Also, the sums $g' + (\ell - 1)h'$ and $g + (\ell - 1)h$ are equal, and therefore have equal initial forms. This shows that (g', h') belongs to the set S . On the other hand, because $\text{in}_w(f) = \text{in}_1(\text{in}_w(h))$, $h' = h - f$ has strictly smaller degree than h , which contradicts our choice of (g, h) . \square

Proof of Proposition 10. We first prove the set-wise statement for $\mathbb{k} = \mathbb{R}, \mathbb{C}$. Let K denote the field $\mathbb{k}\{\{t\}\}$. We use the notation $I = I(C)$, $\bar{I} = I(\bar{C})$, $\ell = v \cdot x$, and $\hat{I} = \bar{I} + \langle \ell - 1 \rangle = I(\hat{C})$. Because all the rays are defined over \mathbb{Q} , it suffices to prove that the two sets, $\text{Trop}_{\mathbb{k}}(C)$ and the image of $\text{Trop}_{\mathbb{k}}(\hat{C} \cap (\mathbb{R}_{\leq 0})^{n+1})$, have the same points in \mathbb{Q}^n .

(\supseteq) Suppose $w \in \text{Trop}_{\mathbb{k}}(\hat{C}) \cap (\mathbb{Q}_{\leq 0})^{n+1}$. Then there exists $y = (y_0, \dots, y_n) \in \mathcal{V}_{K^*}(\hat{I})$ with $\text{val}(y) = -w$. By homogeneity, the point $(1, y_1/y_0, \dots, y_n/y_0)$ belongs to $\mathcal{V}_{K^*}(\bar{I})$, meaning that $(y_1/y_0, \dots, y_n/y_0)$ belongs to $\mathcal{V}_{K^*}(I)$. The negative of the valuation of this point is $(w_1 - w_0, \dots, w_n - w_0)$ and belongs to $\text{Trop}_{\mathbb{k}}(C)$.

(\subseteq) Suppose $u \neq 0$ belongs to $\text{Trop}_{\mathbb{k}}(C) \cap \mathbb{Q}^n$. Let $w = (0, u) - \max\{0, u_1, \dots, u_n\}\mathbf{1}$. Then $w \in \text{Trop}(\bar{C}) \cap (\mathbb{Q}_{\leq 0})^{n+1}$ and w has some zero coordinate from the attained maximum and some non-zero coordinate from non-equal coordinates of $w = (0, u)$. Lemma 11 then implies that $\text{in}_w(\ell) = \text{in}_{(0, u)}(\ell)$ does not vanish any point in $\mathcal{V}(\text{in}_w(\bar{I})) \cap (\mathbb{C}^*)^{n+1}$.

Now take $y \in \mathcal{V}_{K^*}(I)$ with $-\text{val}(y) = u$. Then $(1, y)$ belongs to $\mathcal{V}_{K^*}(\bar{I})$ and has $-\text{val}(1, y) = (0, u)$ and $\text{coeff}(1, y) = (1, a)$ for some $a \in (\mathbb{C}^*)^n$. In particular, $(1, a)$ belongs to the variety of the initial ideal $\text{in}_{(0, u)}(\bar{I})$, meaning that $\text{in}_{(0, u)}(\ell)(1, a)$ is not zero. It follows that $\ell(1, y)$ equals $ct^q + \text{higher order terms}$, with leading coefficient $c = \text{in}_{(0, u)}(\ell)(1, a)$ and valuation $q = \min\{0, \text{val}(y_1), \dots, \text{val}(y_n)\} = -\max\{0, u_1, \dots, u_n\}$.

For every $\lambda \in K^*$, the point $(\lambda, \lambda y)$ belongs to $\mathcal{V}_K(\bar{I})$. Let λ equal $1/\ell(1, y)$. Then the point $(\lambda, \lambda y)$ satisfies $\ell(\lambda, \lambda y) = 1$ and belongs to $\mathcal{V}_K(\hat{I})$. Furthermore

$$-\text{val}(\lambda, \lambda y) = -\text{val}(1, y) - \text{val}(\lambda)\mathbf{1} = (0, u) + \text{val}(\ell(1, y))\mathbf{1} = (0, u) - \max\{0, u_1, \dots, u_n\}\mathbf{1} = w.$$

Thus $w \in \text{Trop}_{\mathbb{k}}(\hat{C})$. Also note that $w \in (\mathbb{R}_{\leq 0})^{n+1}$ and $u = (w_1 - w_0, \dots, w_n - w_0)$.

Now we fix $\mathbb{k} = \mathbb{C}$ and show that the multiplicity of w in $\text{Trop}_{\mathbb{C}}(\hat{C})$ equals the multiplicity of $(w_1 - w_0, \dots, w_n - w_0)$ in $\text{Trop}_{\mathbb{C}}(C)$. It is a general commutative algebra fact that if P is a minimal prime of a homogeneous ideal J with multiplicity $\text{mult}(P, J) = m$ and $l(X) \in \mathbb{C}[x_0, \dots, x_n]_1$ is not a zero-divisor modulo J , then $P + \langle l(x) - 1 \rangle$ is a minimal prime of $J + \langle l(x) - 1 \rangle$ with the same multiplicity m .

Applying this with $J = \text{in}_w(\bar{I})$ and $l(x) = x_0$ shows that the multiplicity of a ray \vec{u} in $\text{Trop}_{\mathbb{C}}(I)$ equals the multiplicity of the cone $\mathbb{R}_+(0, u) + \mathbb{R}\mathbf{1}$ in $\text{Trop}_{\mathbb{C}}(\bar{I})$. On the other hand, by Lemmas 11 and 12, we can also apply this with $l(x) = \text{in}_w(\ell)$. Note that since w belongs to $(\mathbb{R}_{\leq 0})^{n+1} \cap \text{Trop}_{\mathbb{C}}(\ell - 1)$, we have that $\text{in}_w(\ell - 1) = \text{in}_w(\ell) - 1$. This shows that the multiplicity of a ray $\vec{w} \in \text{Trop}(\hat{C})$ is that same as the multiplicity of $\vec{w} + \mathbb{R}\mathbf{1}$ in $\text{Trop}_{\mathbb{C}}(\bar{I})$. Putting these together, that a ray $w \in \text{Trop}_{\mathbb{C}}(\hat{I}) \cap (\mathbb{R}_{\leq 0})^{n+1}$ has the same multiplicity as the ray of $(w_1 - w_0, \dots, w_n - w_0)$ in $\text{Trop}_{\mathbb{C}}(I)$. \square

This allows us to compute $\text{Trop}_{\mathbb{k}}(C)$ by computing $\text{Trop}_{\mathbb{k}}(\hat{C}) \cap (\mathbb{R}_{\leq 0})^{n+1}$. As described in the next section, the benefit of focusing on rays with nonpositive coordinates is that they correspond to paths in a variety with coordinates approaching zero, rather than infinity.

3 Algorithms

The following describes algorithms for computing complex and real tropical curves. These algorithms use local uniformization of complex curves, e.g. [24, Thm. A.3.2], to transform Puiseux series into power series, which allows us to compute valuations and multiplicities using Cauchy integrals. Given a curve $C \subset \mathbb{C}^n$ with corresponding curve $\hat{C} \subset \mathbb{C}^{n+1}$ which is the intersection of the closure of C in \mathbb{P}^n and an affine coordinate patch satisfying (3), a rough outline of our strategy for computing its tropicalization is as follows:

1. As defined in Section 3.1.1, compute a point τ_j in the endgame operating zone of \hat{C} with respect to x_j for $j = 0, \dots, n$.
2. As described in Section 3.1.2, for each point $p \in \hat{C}$ with some zero coordinate $p_j = 0$ and continuous path $P(s)_{s \in [0, 1]} \subset \hat{C}$ such that $P_j(s) = \tau_j \cdot s$, compute an analytic reparametrization of $P(s)$ and use Cauchy integrals to compute the valuation of a power series expansion of each coordinate.
3. Collect all valuations with appropriate multiplicities to obtain $\text{Trop}(C)$.

The algorithms for computing $\text{Trop}_{\mathbb{C}}(C)$ (Section 3.2) and $\text{Trop}_{\mathbb{R}}(C)$ (Section 3.3) rely on computations that are common to both. For ease of exposition, we break these into separate algorithms, which are discussed in Section 3.1.

3.1 Algorithms common to \mathbb{C} and \mathbb{R}

There are two sub-algorithms which are common to both the complex and real algorithms. First, we describe how to ensure that we are inside the radius of convergence of the Puiseux series, which is called the *endgame operating zone*, e.g., see [24, §10.3.1]. Once inside the endgame operating zone, we next describe computing valuations and multiplicities via Cauchy's integral formula after computing a uniformization. These two algorithms are essential in our approach for computing complex and real tropical curves.

3.1.1 Finding the endgame operating zone

A main tool in the computations below is the parametrization of a curve $X \subset \mathbb{C}^{n+1}$ in a neighborhood of a point $p \in X$. One can parametrize a branch of the curve around this point by the value of some variable, say $x_j = s$. Each of the other coordinates are then locally functions of s that can be expressed as Puiseux series. To be meaningful, the computations below must take place in the radius of convergence of these Puiseux series. The domain of convergence of all the Puiseux series of the coordinates of a curve around a point is called the **endgame operating zone**. This zone is calculated by computing the critical points with respect to the parameterizing variable x_j . Explicitly, suppose that X is an irreducible curve not contained in any coordinate hyperplane and $f = (f_1, \dots, f_n) \in (\mathbb{k}[x_0, \dots, x_n])^n$ is a polynomial system such that X is an irreducible component of the solution set of $f = 0$ which has multiplicity 1 with respect to f . The set of critical points of X with respect to x_j and f is the set of $x \in X$ for which $Jf(x)_{\hat{j}}$ has a nonzero null vector. Here we use $Jf(x)_{\hat{j}}$ to denote the Jacobian matrix of f evaluated at x with the j^{th} column removed.

In Algorithm 1, we actually compute a smaller threshold to simplify the computation of the real tropical curve, as we will see in Section 3.3.

Input : An irreducible curve $X \subset \mathbb{C}^{n+1}$ not contained in a coordinate hyperplane and a polynomial system f such that X is an irreducible component of the solution set of $f = 0$ of multiplicity 1; the set $\Lambda \subset \mathbb{C}^{n+1}$ consisting of points $X \cap \mathcal{V}(x_0 \dots x_n)$; index $j \in \{0, \dots, n\}$.

Output: $\tau_j \in \mathbb{R}_{>0}$ such that the disk of radius τ_j centered at any point in Λ is contained in the endgame operating zone of X with respect to x_j .

- 1 Compute the set S of critical points of X with respect to x_j and f , i.e.,
 $S = \{x \in X \mid Jf(x)_{\hat{j}} \text{ has a nonzero null vector}\};$
- 2 Compute $T_j = \{\text{abs}(\pi_j(S))\} \cup \{\text{abs}(\pi_j(\Lambda))\} \subset \mathbb{R}_{\geq 0}$ where $\pi_j(y_0, \dots, y_n) = y_j$;
- 3 Set $T_j^* = T_j \setminus \{0\}$;
- 4 **return** $0 < \tau_j < \min(T_j^*)$, or some arbitrary positive number if T_j^* is empty ;

Algorithm 1: Computing τ_j inside the endgame operating zone of X with respect to x_j .

The following is immediate from the definition of the endgame operating zone.

Proposition 13. *Algorithm 1 returns $\tau_j > 0$ which is inside the endgame operating zone with respect to x_j .*

3.1.2 Computing valuations and multiplicities

Once inside the endgame operating zone, one can use path tracking to compute valuations of a Puiseux series expansion. In Algorithm 2, we compute the primitive integer vector on the ray spanned by the valuation of this Puiseux series. For a curve X , the input consists of a point $p \in X$ such that $p_j = \tau_j$ where τ_j is computed as in Algorithm 1. Then, we consider the path $P(s) \subset X$ parametrized by $P_j(s) = \tau_j s$ for $s \in [0, 1]$ with $P(1) = p$. In particular, this path $P(s)$ is a function of s which corresponds with a convergent Puiseux series.

Input : An irreducible curve $X \subset \mathbb{C}^{n+1}$ not contained in a coordinate hyperplane;
 $j \in \{0, \dots, n\}$; $\tau \neq 0$ inside of the endgame operating zone of X with respect to j ; and a point $p \in X$ such that $p_j = \tau$ which defines the path
 $P(s) \in X \cap \mathcal{V}(x_j - \tau s)$ for $s \in [0, 1]$ where $P(1) = p$.

Output: The primitive vector in $\mathbb{Z}_{\geq 0}^{n+1}$ of the ray spanned by the valuation of $P(s)$.

- 1 Compute cycle number c of the path $P(s)$;
- 2 **for** k from 0 to n **do**
- 3 Initialize with $u_k = -1$ and $a = 0$;
- 4 **while** $a = 0$ **do**
- 5 Update $u_k \leftarrow u_k + 1$;
- 6 Update $a \leftarrow \int_0^{2\pi} P_k(e^{c \cdot i\theta}) / (e^{i\theta})^{u_k} d\theta$;
- 7 Set $u = (u_0, \dots, u_n) \in \mathbb{Z}_{\geq 0}^{n+1}$;
- 8 Compute $g = \gcd(u)$;
- 9 **return** Primitive vector $r = u/g \in \mathbb{Z}_{\geq 0}^{n+1}$;

Algorithm 2: Computing the primitive vector corresponding to a path valuation.

The following shows that the path $P(s)$ is parametrized by a Puiseux series and that Algorithm 2 correctly computes its valuation.

Proposition 14. *Let $p \in X \subset \mathbb{C}^{n+1}$, j , and τ be the input of Algorithm 2 and $r \in \mathbb{Z}_{\geq 0}^{n+1}$ be the output. Then there is a point $y \in (\mathbb{C}\{\{t\}\})^{n+1}$ in $\mathcal{V}_{\mathbb{C}\{\{t\}\}}(I(X))$ that converges for $t \in [0, 1]$ and satisfies $y(s) = P(s)$ for all $s \in [0, 1]$. The valuation of y is $(1/r_j) \cdot r \in \mathbb{Q}_{\geq 0}^{n+1}$.*

Proof. Since $c > 0$ is the cycle number, local uniformization, e.g., [24, Thm. A.3.2], yields that $s \mapsto P(s^c)$ is analytic with respect to s on a neighborhood of $s = 0$. Because τ was chosen inside the endgame operating zone of C with respect to x_j , this neighborhood contains the unit disk $\{z \in \mathbb{C} \mid |z| \leq 1\}$. Taking power series expansions of each coordinate gives $\tilde{y} \in (\mathbb{K}[[t]]_{\text{conv}})^{n+1}$ with $\tilde{y}(s) = P(s^c)$ for all $|s| \leq 1$.

We claim that u is the valuation of \tilde{y} . To see this, write the k th coordinate as $\tilde{y}_k(t) = \sum_{\ell} a_{\ell} t^{\ell}$ where $a_{\ell} \in \mathbb{C}$. Then for any $\ell \in \mathbb{Z}_{\geq 0}$, the integral $\int_0^{2\pi} P_k(e^{c \cdot i\theta}) / e^{i\ell\theta} d\theta$ equals

the integral $\int_0^{2\pi} \tilde{y}_k(e^{i\theta})/e^{i\ell\theta} d\theta$. By the Cauchy integral formula this integral equals $a_\ell/2\pi$. Algorithm 2 computes $u_k = \text{val}(\tilde{y}_k)$ as the minimum ℓ for which this integral is nonzero.

Now set $y(t) = \tilde{y}(t^{1/c}) \in \mathbb{C}\{\{t\}\}^{n+1}$. Then $\text{val}(y) = (1/c) \text{val}(\tilde{y}) = (1/c)u$. Since \tilde{y} converges for $t \in [0, 1]$, so does y . Furthermore, for $s \in [0, 1]$, we have $y(s) = \tilde{y}(s^{1/c}) = P(s)$. In particular, the j^{th} coordinate of y is $y_j = \tau t$ and $\text{val}(y_j) = 1$. The valuation of y is a multiple of u with j^{th} coordinate 1, meaning that $\text{val}(y) = (1/r_j) \cdot r$. \square

Furthermore, any Puiseux series $y \in \mathcal{V}_{\mathbb{k}\{\{t\}\}_{\text{conv}}}(I(X))$ with non-negative valuations and j^{th} coordinate $y_j = \tau t$ parametrizes such a path in X .

Proposition 15. *Suppose that $y \in \mathcal{V}_{\mathbb{k}\{\{t\}\}_{\text{conv}}}(I(X) + \langle x_j - \tau t \rangle)$ and $\text{val}(y) \in (\mathbb{Q}_{\geq 0})^{n+1}$. Then y converges for $t \in [0, 1]$ and $p = y(1)$ defines a viable input to Algorithm 2.*

Proof. Since y is convergent in a neighborhood of $t = 0$ and τ was chosen inside the endgame operating zone of X with respect to x_j , we know y converges for $s \in (0, 1]$. We see immediately that $p = y(1)$ has j^{th} coordinate $p_j = y_j(1) = \tau$. Since each coordinate y_k has nonnegative valuation, it has a well-defined value at $t = 0$. Therefore $P(s) = y(s)$ defines a continuous path in $X \cap \mathcal{V}(\langle x_j - \tau s \rangle)$ for $s \in [0, 1]$. \square

3.2 Computing complex tropical curves

By using Algorithms 1 and 2, we now present an approach for computing complex tropical curves of an irreducible curve $C \subset (\mathbb{C}^*)^n$, namely Algorithm 3. We assume that we are given a polynomial system f such that C is an irreducible component of the solution set of $f = 0$ which has multiplicity 1 with respect to f . As discussed in Section 2.2, we also start with the irreducible curve $\widehat{C} \subset \mathbb{C}^{n+1}$ with corresponding polynomial system \widehat{f} , i.e., \widehat{C} is an irreducible component of the solution set of $\widehat{f} = 0$ which has multiplicity 1 with respect to \widehat{f} .

Before proving that Algorithm 3 computes the tropical curve of C , we consider an illustrative example that demonstrates the steps of the algorithm.

Example 16. Consider the quartic curve $C \subset \mathbb{C}^2$ defined by $f = x_1^3 x_2 - x_1 x_2^3 + x_1^3 - x_2^2 = 0$, shown in Figure 3. Its homogenization $\bar{f} = x_1^3 x_2 - x_1 x_2^3 + x_0 x_1^3 - x_0^2 x_2^2$ defines a curve $\bar{C} \subset \mathbb{P}^2$, and the vector $v = (1, 1, 2)$ satisfies the condition (3). Thus, $\widehat{C} \subset \mathbb{C}^3$ is the curve defined by $\bar{f} = 0$ and $x_0 + x_1 + 2x_2 = 1$. The set Λ consists of the five intersection points of \widehat{C} with $\mathcal{V}(x_0 x_1 x_2)$. We partition the points by their first zero coordinate:

$$\Lambda_0 = \{(0, 1, 0), (0, 1/3, 1/3), (0, 0, 1/2), (0, -1, 1)\}, \quad \Lambda_1 = \{(1, 0, 0)\}, \quad \text{and} \quad \Lambda_2 = \emptyset.$$

For each $j = 0, 1, 2$, Algorithm 1 computes $\tau_j > 0$ inside the endgame operating zone by calculating the projections of the points Λ onto each coordinate and the values $t \in \mathbb{C}$ at which the plane $x_j - t$ is tangent to the curve \widehat{C} . For $j = 0$ the minimum of non-zero absolute value of these numbers is $\min(T_0^*) \approx 0.2162$. Indeed, as seen in Figure 3, the plane $x_0 = -\min(T_0^*)$ is tangent to \widehat{C} . For $j = 1$, we find $\min(T_1^*) \approx 0.2483$, which is attained by a complex tangency. We take τ_j to be any positive number less than $\min(T_j^*)$, for example $\tau_0 = \tau_1 = 0.1$. Then, the paths defined by the intersection of \widehat{C} and a disk of radius τ_j around each point in Λ_j correspond with convergent Puiseux series.

Input : An irreducible curve $C \subset (\mathbb{C}^*)^n$; a polynomial system f such that C is an irreducible component of multiplicity one of the solution set $f = 0$; and a vector $v \in (\mathbb{C}^*)^{n+1}$ satisfying condition (3).

Output: $\text{Trop}_{\mathbb{C}}(C)$, a collection of primitive vectors in \mathbb{Z}^n with multiplicity.

```

1 Initialize  $\text{Trop}_{\mathbb{C}}(C) = \emptyset$  ;
2 Define  $\widehat{C} = \overline{C} \cap \mathcal{V}(v \cdot x - 1)$  and  $\widehat{f} = \overline{f} \cup \{v \cdot x - 1\}$  ;
3 Set  $\Lambda = \widehat{C} \cap \mathcal{V}(x_0 \cdot x_1 \cdots x_n)$ ;
4 Partition  $\Lambda = \sqcup_j \Lambda_j$ , where  $\Lambda_j = \{x \in \Lambda \mid x_0, \dots, x_{j-1} \neq 0, x_j = 0\}$  ;
5 for  $j$  from 0 to  $n$  do
6   if  $\Lambda_j = \emptyset$  then
7     | Continue ;
8   Call Algorithm 1 using  $\widehat{C}$ ,  $\widehat{f}$ ,  $\Lambda$ , and  $j$  yielding  $\tau_j > 0$  ;
9   Compute  $C_j^\tau = \widehat{C} \cap \mathcal{V}(x_j - \tau_j) \subset \mathbb{C}^{n+1}$  ;
10  Compute  $\Lambda_j^\tau$  which consists of  $p \in C_j^\tau$  such that the path starting, with  $s = 1$ , at  $p$ 
    defined by  $\widehat{C} \cap \mathcal{V}(x_j - \tau_j s)$  for  $s \in [0, 1]$  ends at a point in  $\Lambda_j$  ;
11  for each  $p \in \Lambda_j^\tau$  do
12    Call Algorithm 2 using  $\widehat{C}$ ,  $j$ ,  $\tau_j$ , and  $p$  yielding  $r \in \mathbb{Z}_{\geq 0}^{n+1}$ ;
13    Add  $(r_0 - r_1, \dots, r_0 - r_n)$  to  $\text{Trop}_{\mathbb{C}}(C)$  with multiplicity contribution  $1/r_j$ ;
14 return  $\text{Trop}_{\mathbb{C}}(C)$  ;

```

Algorithm 3: Computation of $\text{Trop}_{\mathbb{C}}$

For each $j = 0, 1, 2$, we track points limiting to the points in $\Lambda_j \subset \mathcal{V}(x_j)$. For example, for $j = 0$, we compute $C_0^\tau = \widehat{C} \cap \mathcal{V}(x_0 - 0.1)$, which consists of four points in \mathbb{C}^3 , each of which tracks to a unique point in Λ_0 . Therefore $C_0^\tau = \Lambda_0^\tau$. We apply Algorithm 2 to each point $p \in \Lambda_0^\tau$. The point $p \approx (0.1, -0.022, 0.461) \in \Lambda_0^\tau$ defines a path $P(s) \in \widehat{C} \cap \mathcal{V}(x_0 - 0.1s)$ with $P(1) = p$ and $P(0) = (0, 0, 1/2)$. The cycle number of this path is $c = 1$, meaning that the map $z \mapsto P(z)$ is analytic for $|z| \leq 1$. In particular, each coordinate $g_j(z) = P_j(z)$ has a power series expansion in z . Using Cauchy's integral formula, we can find the leading term in this power series. By definition $g_0(z) = 0.1z$. For $g_1(z) = P_1(z)$, we use numerical integration to calculate that

$$\frac{g_1^{(k)}(0)}{k!} = \frac{1}{2\pi} \int_0^{2\pi} \frac{g_1(0.1e^{i\theta})}{(0.1e^{i\theta})^k} d\theta = 0 \quad \text{for } k = 0, 1, \text{ and } \frac{g_1^{(2)}(0)}{2!} = \frac{1}{2\pi} \int_0^{2\pi} \frac{g_1(0.1e^{i\theta})}{(0.1e^{i\theta})^2} d\theta = -0.02.$$

Therefore, the leading term of the power series expansion of $g_1(z)$ is $\frac{g_1^{(2)}(0)}{2!} z^2 = -0.02z^2$. Similarly, we see that $g_2(z) = 1/2 + \text{higher degree terms}$. Therefore Algorithm 2 outputs $r = (1, 2, 0)$. This contributes $(r_0 - r_1, r_0 - r_2) = (-1, 1)$ to $\text{Trop}_{\mathbb{C}}(C)$ with multiplicity 1.

On the other hand, for $j = 1$, $C_1^\tau = \widehat{C} \cap \mathcal{V}(x_1 - 0.1)$ consists of four points in \mathbb{C}^3 , two of which are complex and limit to the point $(0, 0, 1/2) \in \Lambda_0$, two of which are real and track to $(1, 0, 0) \in \Lambda_1$. The latter two are Λ_1^τ . The point $p \approx (0.8293, 0.1, 0.0354) \in \Lambda_1^\tau$ defines a path $P(s) \in \widehat{C} \cap \mathcal{V}(x_1 - 0.1s)$ with $P(1) = p$ and $P(0) = (1, 0, 0)$. The cycle number of this path is $c = 2$, meaning that the map $z \mapsto P(z^2)$ is analytic for $|z^2| \leq 1$.

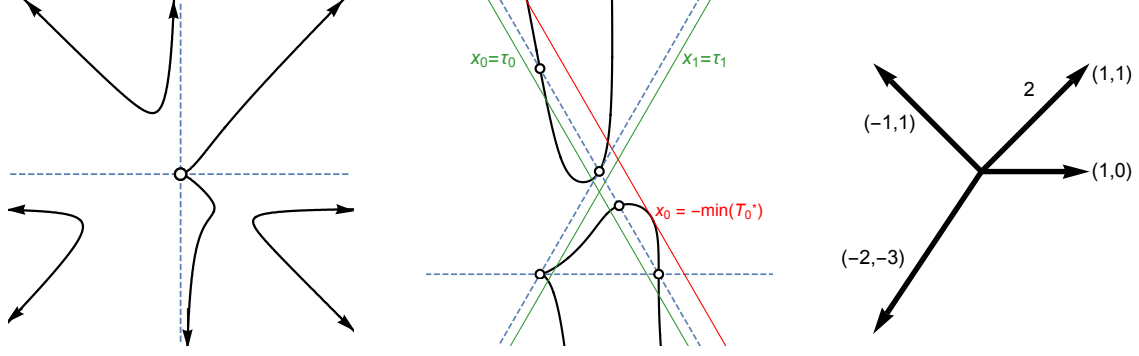


Figure 3: Affine patches C and \widehat{C} of the quartic curve in Example 16 and $\text{Trop}_{\mathbb{C}}(C)$.

As above we use Cauchy's integral formula to compute power series expansions of each coordinate $g_j(z) = P_j(z^2)$, to find $P(z^2) = (1, 0.1z^2, (0.1)^{3/2}z^3) + \text{higher degree terms}$, giving $r = (0, 2, 3)$. This contributes $(r_0 - r_1, r_0 - r_2) = (-2, -3)$ to $\text{Trop}_{\mathbb{C}}(C)$ with multiplicity $1/r_1 = 1/2$. Repeating this process for the second point $p \approx (0.9635, 0.1, -0.0317) \in \Lambda_1^+$ also gives the ray $(-2, -3)$ with multiplicity $1/2$, for total multiplicity of 1. The other rays in $\text{Trop}_{\mathbb{C}}(C)$ are computed similarly, giving the tropical curve in Figure 3.

Theorem 17. *Algorithm 3 computes the primitive vectors with multiplicities of $\text{Trop}_{\mathbb{C}}(C)$.*

Proof. Let \mathcal{T} be the set of vectors with multiplicities computed by Algorithm 3. Suppose that u is a primitive vector of $\text{Trop}_{\mathbb{C}}(C)$ with multiplicity m . By Proposition 10, we know $w = (0, u) - \max\{0, u_1, \dots, u_n\}\mathbf{1}$ is a primitive vector of $\text{Trop}_{\mathbb{C}}(\widehat{C})$ with multiplicity m . Let j be the first index for which $w_j < 0$ and let τ_j be the output of Algorithm 1 with $X = \widehat{C}$. The ray \vec{w} and tropical hyperplane $\text{Trop}_{\mathbb{C}}(\langle x_j - \tau_j t \rangle)$ meet transversely at the point $|1/w_j|w$. By [21, Def. 3.6.11], the multiplicity of $|1/w_j|w$ in $\text{Trop}_{\mathbb{C}}(\widehat{I} + \langle x_j - \tau_j t \rangle)$ equals $m \cdot |w_j|$.

Let $K = \mathbb{C}\{\{t\}\}_{\text{conv}}$. By [21, Prop. 3.4.8], the multiplicity of $|1/w_j|w$ in the tropical variety of $\widehat{I} + \langle x_j - \tau_j t \rangle$ equals the number of points in its variety over K with this valuation,

$$V_w = \left\{ y \in \mathcal{V}_K(\widehat{I} + \langle x_j - \tau_j t \rangle) \mid |\text{val}(y)| = -|1/w_j|w \right\}.$$

By Proposition 15, any $y \in V_w$ converges for $t \in [0, 1]$ and $p = y(1)$ defines a viable input for Algorithm 2. Since $y_j = \tau_j t$, we see that $p \in C_j^r = \widehat{C} \cap \mathcal{V}(x_j - \tau_j)$. Furthermore, since j is the smallest index for which $\text{val}(y_j) > 0$, j is the smallest zero coordinate of $y(0)$. Therefore $y(0)$ belongs to Λ_j and p belongs to Λ_j^r . By Proposition 14, Algorithm 2 returns primitive vector r , where $(1/r_j)r = -|1/w_j|w$ is the valuation of y . Thus, each point in V_w contributes the vector $u = (r_0 - r_1, \dots, r_0 - r_n)$ to \mathcal{T} with multiplicity $1/r_j = 1/|w_j|$. As $\#V_w = m \cdot |w_j|$, the vector u appears in \mathcal{T} with multiplicity at least m . By Proposition 14, every path used in Algorithm 2 comes from some tuple of Puiseux series, giving us equality. \square

Example 18. The curve from Example 9 displayed in Figure 2 demonstrates some of the subtlety in computing the multiplicities of rays in the tropical variety. The cusp at the origin contributes to the ray $(-1, -1)$ in $\text{Trop}_{\mathbb{C}}(f)$ with multiplicity 2.

There are two points in $\mathcal{V}(f) \cap \{x = \tau_j\}$ that track to the origin along this cusp, and each of these paths has cycle number $c = 2$. Re-parametrizing by $x = t^2$ and using Cauchy's integral formula, we find the initial terms of the two corresponding Puiseux series in $\mathcal{V}_{\mathbb{R}\{\{t\}\}}(f)$:

$$(x, y) = \left(t^2, \quad t^2 \pm t^3 + \frac{3}{4} t^4 \pm \frac{45}{32} t^5 + \dots \right),$$

each with $u = \text{val}(1, x, y) = (0, 2, 2)$. Thus, $g = \gcd(u) = 2$. For each of these two paths, Algorithm 2 returns primitive vector $r = u/g = (0, 1, 1)$. In Algorithm 3, each of these paths contributes $(-1, -1)$, each with multiplicity 1, thereby yielding a total contribution of 2.

Remark 19. We highlight some of the key differences between Algorithm 3 and the approach presented [20]. First, Algorithm 3 explicitly computes the endgame operating zone to ensure all computations are performed on convergent Puiseux series. The approach of [20] requires slicing so that the intersection points are within a so-called tentacle. Then, they track these to compute additional points in the same tentacle. By using lattice recovery techniques, they heuristically recover the valuation. Although our implementation as described in Section 4 performs computations which are not certified, these computations are amendable to certification. In our approach, inside the endgame operating zone, we first compute the cycle number. Since this can be performed using a Newton homotopy, this computation can be certifiably computed using [12, 13]. Then, Cauchy's integral theorem is used to compute the valuation. When the Cauchy integral cannot be computed exactly, the use of the trapezoid rule produces an exponentially convergent numerical method [27] for computing the Cauchy integral.

The techniques of [20] could possibly be adapted to compute real tropical curves, but that is not pursued by the authors. Algorithm 3 can be transformed into a method for computing the real tropical curve, as described below.

3.3 Computing real tropical curves

Computing the real tropical curves is similar to that of complex tropical curves except that only paths starting at real points are considered, as presented in Algorithm 4.

Before proving that Algorithm 4 computes the real tropical curve of C , we consider an illustrative example that demonstrates the steps of the algorithm.

Example 20. Consider the quartic curve C of Example 16. The computation of $\text{Trop}_{\mathbb{R}}(C)$ largely follows that of $\text{Trop}_{\mathbb{C}}(C)$. We now must check both sides of the coordinate hyperplanes $\mathcal{V}(x_j)$ for real points. For example, intersecting \widehat{C} with $\mathcal{V}(x_1 - 0.1)$ gives two points that limited to the point $(1, 0, 0)$. However there are no real points in $\widehat{C} \cap \mathcal{V}(x_1 + 0.1)$ that limit to $(1, 0, 0)$, so C_1^- is empty. Indeed, tracking the point $p \approx (0.8293, 0.1, 0.0354) \in \Lambda_1^+$ along the path $\widehat{C} \cap \mathcal{V}(x_1 - 0.1e^{i\theta})$ for $\theta \in [0, \pi]$ yields a complex point in $\widehat{C} \cap \mathcal{V}(x_1 + 0.1)$. As in Example 16, applying Algorithm 2 to the point p gives ray $r = (0, 2, 3)$. Every coordinate of p is positive, so we add the ray $(r_0 - r_1, r_0 - r_2) = (-2, -3)$ to $\text{Trop}_{\mathbb{R}}(I)$ with sign vector $(+, +)$. The other point $p \approx (0.9635, 0.1, -0.0317) \in \Lambda_1^+$ gives $(-2, -3) \in \text{Trop}_{\mathbb{R}}(I)$ with sign vector $(+, -)$. Repeating this process for the points in Λ_0^+ , gives the signed real tropical variety $\text{Trop}_{\mathbb{R}}(C)$ in Figure 4.

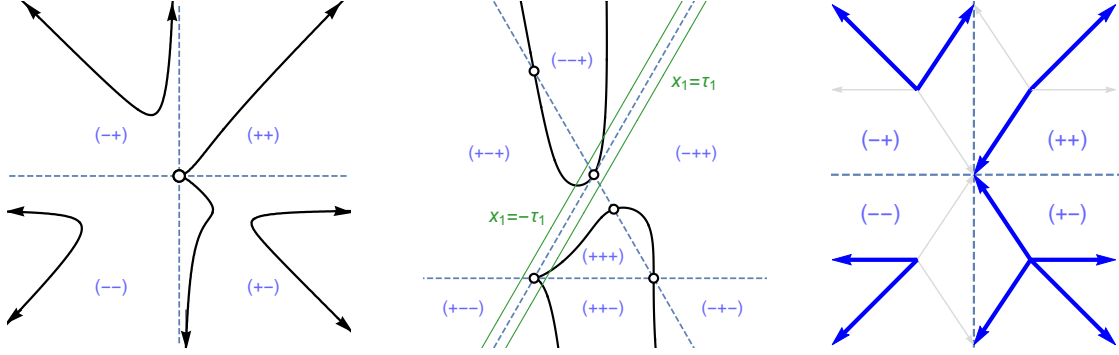


Figure 4: Affine curves C and \widehat{C} of the real quartic in Example 20 and the signed real tropical variety $\text{Trop}_{\mathbb{R}}(C)$ contained in reflected copies of $\text{Trop}_{\mathbb{C}}(C)$.

Input : A real irreducible curve $C \subset (\mathbb{C}^*)^n$ with $C \cap (\mathbb{R}^*)^n \neq \emptyset$; a polynomial system f such that C is an irreducible component of multiplicity one of the solution set $f = 0$; and a vector $v \in (\mathbb{R}^*)^{n+1}$ satisfying condition (3).

Output: $\text{Trop}_{\mathbb{R}}(C)$, a collection of primitive vectors in \mathbb{Z}^n with signs $\{\pm 1\}^n$.

```

1 Define  $\widehat{C} = \overline{C} \cap \mathcal{V}(v \cdot x - 1)$  and  $\widehat{f} = \overline{f} \cup \{v \cdot x - 1\}$  ;
2 Set  $\Lambda = \widehat{C} \cap \mathcal{V}(x_0 \cdot x_1 \cdots x_n)$ ;
3 if  $\Lambda = \emptyset$  then
4   | return  $\text{Trop}_{\mathbb{R}}(C) = \{0\}$  ;
5 Initialize  $\text{Trop}_{\mathbb{R}}(C) = \emptyset$  ;
6 Partition  $\Lambda = \sqcup_j \Lambda_j$ , where  $\Lambda_j = \{x \in \Lambda \mid x_0, \dots, x_{j-1} \neq 0, x_j = 0\}$  ;
7 for  $j$  from 0 to  $n$  do
8   | if  $\Lambda_j = \emptyset$  then
9     | Continue ;
10  | Call Algorithm 1 using  $\widehat{C}$ ,  $\widehat{f}$ ,  $\Lambda$ , and  $j$  yielding  $\tau_j > 0$  ;
11  | Compute  $C_j^+ = \widehat{C} \cap \mathcal{V}(x_j - \tau_j) \cap \mathbb{R}^{n+1}$  and  $C_j^- = \widehat{C} \cap \mathcal{V}(x_j + \tau_j) \cap \mathbb{R}^{n+1}$  ;
12  | Compute  $\Lambda_j^+$  which consists of  $p \in C_j^+$  such that the path starting with  $s = 1$ 
    |   at  $p$  defined by  $\widehat{C} \cap \mathcal{V}(x_j - \tau_j s)$  for  $s \in [0, 1]$  ends at a point in  $\Lambda_j$  ;
13  | for each  $p \in \Lambda_j^+$  do
14    |   Call Algorithm 2 using  $\widehat{C}$ ,  $j$ ,  $\tau_j$ , and  $p$  yielding  $r \in (\mathbb{Z}_{\geq 0})^{n+1}$ ;
15    |   Add  $(r_0 - r_1, \dots, r_0 - r_n)$  to  $\text{Trop}_{\mathbb{R}}(C)$  with sign  $(\text{sign}(p_0 p_1), \dots, \text{sign}(p_0 p_n))$ 
16  | Compute  $\Lambda_j^-$  which consists of  $p \in C_j^-$  such that the path starting with  $s = 1$ 
    |   at  $p$  defined by  $\widehat{C} \cap \mathcal{V}(x_j + \tau_j s)$  for  $s \in [0, 1]$  ends at a point in  $\Lambda_j$  ;
17  | for each  $p \in \Lambda_j^-$  do
18    |   Call Algorithm 2 using  $\widehat{C}$ ,  $j$ ,  $-\tau_j$ , and  $p$  yielding  $r \in (\mathbb{Z}_{\geq 0})^{n+1}$  ;
19    |   Add  $(r_0 - r_1, \dots, r_0 - r_n)$  to  $\text{Trop}_{\mathbb{R}}(C)$  with sign  $(\text{sign}(p_0 p_1), \dots, \text{sign}(p_0 p_n))$ 
20 return  $\text{Trop}_{\mathbb{R}}(C)$  ;

```

Algorithm 4: Computation of $\text{Trop}_{\mathbb{R}}$.

Theorem 21. *Algorithm 4 computes the primitive vectors with signs of $\text{Trop}_{\mathbb{R}}(C)$.*

Proof. Let \mathcal{T} be the set of vectors with signs computed by Algorithm 4. Suppose that u is a primitive vector of $\text{Trop}_{\mathbb{R}}(C)$ with sign $\sigma \in \{\pm 1\}^n$. By Proposition 10, we have that $w = (0, u) - \max\{0, u_1, \dots, u_n\}\mathbf{1}$ is a primitive vector of $\text{Trop}_{\mathbb{R}}(\widehat{C})$. The proof of Proposition 10 shows that we can take w with sign $(\lambda, \lambda\sigma)$ for some $\lambda \in \{\pm 1\}$. Let j be the first index for which $w_j < 0$ and let τ_j be the output of Algorithm 1 with $X = \widehat{C}$.

Let $K = \mathbb{R}\{\{t\}\}_{\text{conv}}$. Then there is some point $y \in V_K(\widehat{I} + \langle x_j \pm \tau_j t \rangle)$ with valuation $-|1/w_j|w$ and sign $(\lambda, \lambda\sigma)$. In particular, $y_j = \lambda\sigma_j \cdot \tau_j t$. By Proposition 15, y converges for $t \in [0, 1]$ and $p = y(1)$ and $\tau = \lambda\sigma_j \cdot \tau_j$ defines a viable input for Algorithm 2. As in the proof of Theorem 17, p belongs to C_j^+ and Λ_j^+ if $\lambda\sigma_j = 1$, and p belongs to C_j^- and Λ_j^- if $\lambda\sigma_j = -1$. By Proposition 14, Algorithm 2 returns primitive vector r , where $(1/r_j)r = -|1/w_j|w$ is the valuation of y . Thus the vector $u = (r_0 - r_1, \dots, r_0 - r_n)$ is added to \mathcal{T} with sign vector $\text{sign}(p_0 p_1, \dots, p_0 p_n)$. To see that $\text{sign}(p_0 p_1, \dots, p_0 p_n) = \text{sign}(y_0 y_1, \dots, y_0 y_n) = \sigma$, note that for all $s \in (0, 1]$ and any $k = 0, \dots, n$, the coordinate function $y_k(s)$ is non-zero and therefore has constant sign. If not, then $y_k(s) = 0$ for some $0 < s \leq 1$, then $y(s) \in \Lambda$ and $\tau_j s = |y_j(s)| \in \text{abs}(\pi_j(\Lambda))$, which contradicts our choice of $\tau_j < \text{abs}(\pi_j(\Lambda))$ computed by Algorithm 1. Therefore $\text{Trop}_{\mathbb{R}}(C)$ is contained in \mathcal{T} . By Proposition 14, every path used in Algorithm 2 comes from some tuple of Puiseux series yielding equality. \square

4 Implementation

We have implemented the algorithms from Section 3 using a combination of Matlab and Bertini [7], which is available at [10]. This section briefly summarizes the key steps with respect to implementing the algorithms in Section 3.

4.1 Witness sets

The input, namely an irreducible curve $C \subset (\mathbb{C}^*)^n$, is represented by a *witness set* (see, e.g., [24, Chap. 13] for more details). A witness set for the curve C is a triple $\{f, \mathcal{H}, W\}$ where:

1. f is a polynomial system such that C is an irreducible component of the zero set of f ,
2. \mathcal{H} is a general hyperplane in \mathbb{C}^n , and
3. $W = C \cap \mathcal{H}$.

In this context, a general hyperplane \mathcal{H} is a hyperplane that intersects C transversely, i.e., $C \cap \mathcal{H} \subset (\mathbb{C}^*)^n$ consists of $\deg(C)$ distinct points.

The use of witness sets allows for the restriction of computations to the irreducible curve inside the zero set of f of interest. Moreover, one can easily produce a witness set for $\widehat{C} \subset \mathbb{C}^{n+1}$ as described in Section 2.2 from a witness set for C .

If C has multiplicity > 1 with respect to f , then one can utilize deflation techniques for positive-dimensional components which do not add auxiliary variables, e.g., [14, 18], to reduce to the multiplicity 1 case.

4.2 Implementation of Algorithm 1

The key to Algorithm 1 is in the computation of the set S consisting of critical points. Following the notation of Section 3.1.1, we first compute the set $R \subset X \times \mathbb{P}^{n-1}$ which solves

$$\begin{bmatrix} f(x) \\ Jf(x)_{\hat{j}} \cdot \nu \end{bmatrix} = 0 \quad (5)$$

Recall that $Jf(x)_{\hat{j}}$ denotes the Jacobian matrix of f evaluated at x with the j^{th} column removed. In particular, since X has multiplicity 1 with respect to f , the set $S = \pi(R)$ is a finite set where $\pi(x, \nu) = x$.

By starting with a witness set for X , regeneration [15, 19] can be used to compute R . Moreover, the returned value of Algorithm 1 in our implementation is $\tau_j = \min(T_j^*)/2$ when $T_j^* \neq \emptyset$ and $\tau_j = 1/10$ otherwise.

4.3 Implementation of Algorithm 2

The two key steps in Algorithm 2 are computing the cycle number and the Cauchy integral.

Once inside the endgame operating zone, the cycle number the number of loops around $x_j = 0$ (parametrized by $x_j = \tau e^{i\theta}$) necessary to return to the starting point p . The cycle number is therefore at most the degree of curve. By using loops based on regular polygons, this results in tracking using a sequence of so-called Newton homotopies, in which only the value of x_j depends explicitly on the path tracking parameter. These computations can be performed certifiably [12, 13]. By using regular polygons, the data from this computation is reused for the computation of the Cauchy integral which is described next.

By uniformizing via the cycle number, we reduce to power series computations and the coefficients are computed using Cauchy integrals where the integrand is periodic with period 2π . Hence, the trapezoidal rule, which is computed using the data from the regular polygonal paths described above, is exponentially convergent [27]. Due to the exponential convergence, the challenge of deciding if the integral is zero or nonzero is greatly reduced. That is, the exponential convergence allows one to validate this decision by recomputing using the trapezoid rule with more sample points computed more accurately using higher precision arithmetic.

4.4 Implementation of Algorithm 3

The computations performed in Algorithm 3 reduce to tracking solution paths as the hyperplane \mathcal{H} in the witness set for \widehat{C} is deformed. To calculate $\widehat{C} \cap \mathcal{V}(x_0 \cdots x_n)$, we actually compute $\widehat{C} \cap \mathcal{V}(x_j)$ for $j = 0, \dots, n$ and take their union. Each of these is obtained by tracking the solution paths defined by $\widehat{C} \cap (t \cdot \mathcal{H} + (1 - t) \cdot \mathcal{V}(x_j))$ from $t = 1$ to $t = 0$. The computations in Step 10 and Step 11 follow similarly.

4.5 Implementation of Algorithm 4

One key difference between Algorithm 3 and Algorithm 4 is that only *real* points are retained in Algorithm 4. In our implementation, the determination of reality is based on a user-

determined numerical threshold. By recomputing the points more accurately, the imaginary parts should limit to 0 at a commensurate rate. One could also certify reality by using [17].

4.6 Incomplete intersections

When the polynomial system f in a witness set for the curve $C \subset (\mathbb{C}^*)^n$ consists of more than $n - 1$ polynomials, the standard approach in numerical algebraic geometry is to replace f by a randomization of the form $A \cdot f$. For example, the twisted cubic curve $C \subset \mathbb{C}^3$ is defined by the polynomial system $f = \{y - x^2, z - xy, y^2 - xz\}$. The zeros set of the sufficiently general randomization, say $g = \{y - x^2 + 2(y^2 - xz), z - xy + 3(y^2 - xz)\}$, consists of C and a line. In particular, one virtue of working with witness sets is that one can replace f by g in a witness set for C . Our implementation relies upon the user to provide a randomization.

4.7 Computational challenges

In our experience, the majority of the computational time in computing $\text{Trop}_{\mathbb{C}}$ and $\text{Trop}_{\mathbb{R}}$ using Algorithm 3 and Algorithm 4, respectively, is in the computation of τ_j via Algorithm 1.

Another issue is that endpoints that lie on a coordinate axis are frequently singular, as noted in [20]. By using endgame methods, such as Cauchy's endgame [23], with adaptive precision computations [6], one is able to accurately compute such endpoints. This can be computationally expensive due to the numerical ill-conditioning near singular solutions.

5 Non-planar examples

In this section, we compute the tropicalizations of real and complex curves in more than two dimensions. In our first example, we replicate the main example from [20] and extend it to the real numbers. Our second example is the central curve of a linear program that formed part of the recent counterexample to the continuous Hirsch conjecture [2].

5.1 A -polynomial of a knot

First, we consider the real and complex tropical varieties of a curve whose image under a monomial map is the plane curve defined by the A -polynomial for the knot 8_1 . This curve is the main example of [20] and is a component of the reducible variety defined by the ideal

$$I = \langle z_1 + w_1 - 1, z_2 + w_2 - 1, z_3 + w_3 - 1, z_4 + w_4 - 1, z_5 + w_5 - 1, \\ w_2 w_4 - z_2 z_4 w_1 w_5, z_2 z_4 z_5^2 w_1^2 - z_1^2 w_2 w_3 w_4 w_5, w_3^2 - z_3^2 w_1, w_5^2 - z_2 z_4 z_5^2 \rangle. \quad (6)$$

The set $\mathcal{V}_{\mathbb{C}^*}(I)$ consists of a degree 22 curve C of interest. We note that $\mathcal{V}_{\mathbb{C}}(I)$ also contains 4 additional curves, each having degree 3 and multiplicity greater than one. Algorithms 3 and 4 compute the complex and real tropical varieties of C , consisting of eight and seven rays, respectively, as summarized below:

complex multiplicity	real contribution to complex multiplicity	primitive element of ray in $\text{Trop}(I)$
3	3	(0, 1, 0, -1, 1, 0, 1, 0, 0, 0, 1)
4	2	(-1, 1, 0, 1, -1, 0, 1, 0, 1, 0)
3	3	(0, -1, 0, 1, 1, 0, 0, 0, 1, 1)
1	1	(0, 0, 0, -2, 0, -4, -7, -2, 0, -1)
1	1	(0, -2, 0, 0, 0, -4, 0, -2, -7, -1)
2	2	(2, -2, -1, 0, 0, 2, 0, 0, -1, -1)
2	2	(2, 0, -1, -2, 0, 2, -1, 0, 0, -1)
2	0	(-2, 1, 2, 1, -1, 0, 1, 2, 1, 0)

The complex tropical variety replicates Example 4.1 in [20]. Of the fourteen intersection points of the corresponding curve \widehat{C} with the union of the coordinate hyperplanes, twelve are real. Two of these points have the form $(h, z, w) = (0, 0, -1, 0, -a, 0, 0, 1, 0, a, 0)$, where h is the added homogenizing variable and a satisfies $a^4 - 2a^3 - 5a^2 - 2a + 1 = 0$. Both of these real points contribute one towards the multiplicity of the ray $\text{val}(h, z, w) = (1, 2, 0, 1, 0, 2, 1, 0, 1, 0, 1)$, which corresponds to the second ray listed in the table above. The two complex values of a solving the quartic equation above also contribute one each to the complex multiplicity of this ray, giving a total complex multiplicity of four.

5.2 The central curve of a linear program

In a recent series of papers, Allamigeon, Benchimol, Gaubert, and Joswig [2, 3] develop a theory of tropical linear programming. Among other things, this enabled them to produce a counterexample to the continuous Hirsch conjecture regarding the total curvature of the central path of a linear program.

The central path of a linear program is a segment of an algebraic curve, called the central curve, which joins the analytic center of the feasible polytope and its optimal vertex [8, 11]. A family of linear programs was presented in [2] whose central paths have total curvature that grows exponentially. We compute the real tropical curve of the central curve of one member of this family, specifically, the linear program from [2, §4] with $r = 1$, $t = 4$:

$$\begin{aligned} \text{minimize } v_0 \quad \text{subject to } & -u_0 + t \geq 0, \quad -v_0 + t^2 \geq 0, \quad u_1 \geq 0, \quad v_1 \geq 0, \\ & t^{1/2}(u_0 + v_0) - v_1 \geq 0, \quad tu_0 - u_1 \geq 0, \quad tv_0 - u_1 \geq 0. \end{aligned}$$

The central curve of this linear program is the projection of a curve in \mathbb{R}^{18} with 14 auxiliary variables $(x, s) = (x_1, \dots, x_7, s_1, \dots, s_7)$ defined by the ideal

$$\begin{aligned} I = \langle & x_1s_1 - x_2s_2, \quad x_1s_1 - x_3s_3, \quad x_1s_1 - x_4s_4, \quad x_1s_1 - x_5s_5, \quad x_1s_1 - x_6s_6, \quad x_1s_1 - x_7s_7, \\ & -u_0 + t - x_1, \quad -v_0 + t^2 - x_2, \quad u_1 - x_3, \quad v_1 - x_4, \quad t^{1/2}(u_0 + v_0) - v_1 - x_5, \quad tu_0 - u_1 - x_6, \\ & tv_0 - u_1 - x_7, \quad s_1 - t^{1/2}s_5 - ts_6, \quad s_2 - t^{1/2}s_5 - ts_7 - 1, \quad s_3 - s_6 - s_7, \quad s_4 - s_5 \rangle. \end{aligned} \quad (7)$$

The system consists of 18 variables and 17 equations. The algebraic variety of this ideal consists of two linear 3-spaces, five planes, four lines, and a degree 10 curve, say C . The linear components belong to the *disjoint support variety* described in [11, §7].

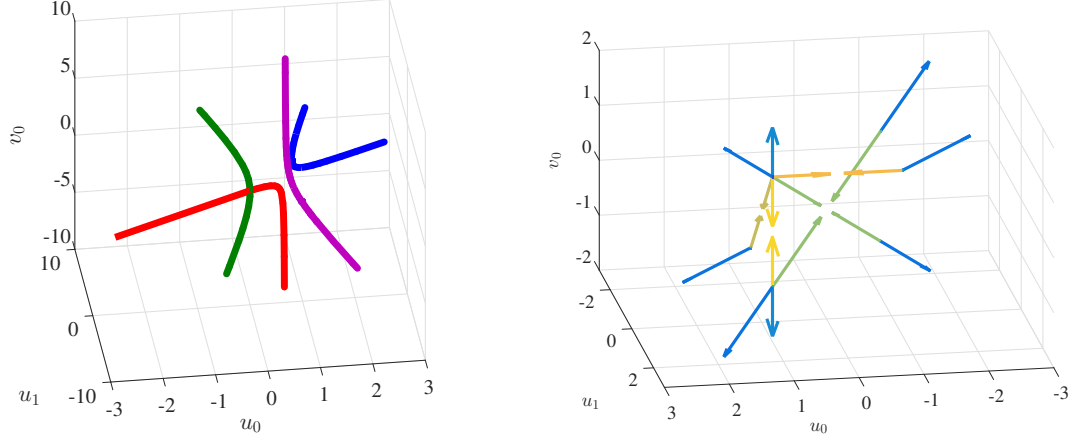


Figure 5: Left: The projection of the degree 10 central curve defined by (7) in Example 5.2 onto the coordinates (u_0, u_1, v_0) . Right: Corresponding signed real tropical variety.

Let \widehat{C} be the curve corresponding to C as in Section 2.2. The total number of points contained in the intersection of \widehat{C} with the union of the coordinate hyperplanes is 22, all of which are real. There is a distinct path through each of these 22 points with cycle number one and each point gives a single contribution to the multiplicity of a ray in the complex tropical curve. In particular, the real and complex tropical curves are equal:

multiplicity	primitive element of ray in $\text{Trop}(I)$ in $(x, s, u_0, v_0, u_1, v_1)$
6	(0, 0, 0, 0, 0, 0, 0, 0, 1, 1, 1, 1, 1, 1, 0, 0, 0, 0)
3	(1, 1, 1, 1, 1, 1, 1, 0, 0, 0, 0, 0, 0, 0, 1, 1, 1, 1)
1	(0, 1, 0, 1, 1, 0, 1, 1, 0, 1, 0, 0, 1, 0, 0, 1, 0, 1)
1	(-1, 0, 0, 0, 0, -1, -1, 0, -1, -1, -1, -1, 0, 0, 0, 0, 0, 0)
2	(-1, 0, 0, -1, -1, 0, 0, 0, -1, -1, 0, 0, -1, -1, 0, 0, 0, -1)
4	(0, -1, 0, 0, 0, 0, 0, -1, 0, -1, -1, -1, -1, -1, 0, 0, 0, 0)
2	(0, 0, -1, -1, -1, -1, -1, -1, 0, 0, 0, 0, 0, 0, -1, -1, -1, -1)
1	(0, 0, -1, 0, 0, 0, -1, -1, -1, 0, -1, -1, -1, 0, 0, -1, -1, 0)
1	(0, 0, 0, 0, 0, 0, 0, 0, 0, 0, 0, 0, 0, 0, 0, -1, 0, 0)
1	(0, 0, 0, 0, 0, 0, 0, 0, 0, 0, 0, 0, 0, 0, 0, 0, -1, 0)

Figure 5 shows a projection of the real points in C and the corresponding signed real tropical curve onto coordinates (u_0, u_1, v_0) . The colors of the real curve indicate the image of connected components. There is an intersection between the green and red segments, but the magenta and blue segments do not intersect.

Generally, the signed real tropical variety of the central curve of a linear program should be closely related to the oriented matroid associated with the input data [5].

6 Conclusion

This paper and its predecessors [16, 20] demonstrate the potential for using the tools of numerical algebraic geometry to compute tropical varieties. The recent expansion of numer-

ical tools for real varieties makes numerical algebraic geometric methods particular effective for computing real tropical varieties. The next natural step for the development of these techniques is to compute tropicalizations of real and complex surfaces.

One important motivation for computing tropical surfaces is that it would enable the computation of tropical curves defined by polynomials with non-constant coefficients, which are of interest for many of the applications mentioned earlier, e.g., [2, 29]. Real tropical surfaces also provide significantly more subtleties than curves. For example, the real tropical variety of a surface may not be pure-dimensional and may not be a sub-fan of the complex tropical variety. With recent developments related to numerically decomposing real surfaces in any dimension, e.g., [9], we are optimistic that a few new ideas building on the ability to compute real tropical curves will be enough to compute real tropical surfaces.

Acknowledgments

DAB and JDH were partially supported by Sloan Research Fellowship and NSF ACI-1460032. CV was partially supported by NSF grant DMS-1204447 and the FRPD program at North Carolina State University. We would like to thank Anton Leykin for helpful comments.

References

- [1] D. Alessandrini. Logarithmic limit sets of real semi-algebraic sets. *Adv. Geom.*, 13(1):155–190, 2013.
- [2] X. Allamigeon, P. Benchimol, S. Gaubert, and M. Joswig. Long and winding central paths. [arXiv:1405.4161](https://arxiv.org/abs/1405.4161), 2014.
- [3] X. Allamigeon, P. Benchimol, S. Gaubert, and M. Joswig. Tropicalizing the simplex algorithm. *SIAM J. Discrete Math.*, 29(2):751–795, 2015.
- [4] F. Ardila, C. Klivans, and L. Williams. The positive Bergman complex of an oriented matroid. *European J. Combin.*, 27(4):577–591, 2006.
- [5] A. Bachem and W. Kern. *Linear Programming Duality: An Introduction to Oriented Matroids*. Universitext. Springer Berlin Heidelberg, 1992.
- [6] D.J. Bates, J.D. Hauenstein, A.J. Sommese, and C.W. Wampler. Adaptive multiprecision path tracking. *SIAM J. Numer. Anal.*, 46(2):722–746, 2008.
- [7] D.J. Bates, J.D. Hauenstein, A.J. Sommese, and C.W. Wampler. Bertini: Software for numerical algebraic geometry. Available at bertini.nd.edu.
- [8] D.A. Bayer and J.C. Lagarias. The nonlinear geometry of linear programming. II. Legendre transform coordinates and central trajectories. *Trans. Amer. Math. Soc.*, 314(2):527–581, 1989.

- [9] D.A. Brake, D.J. Bates, W. Hao, J.D. Hauenstein, A.J. Sommese, and C.W. Wampler. Bertini_real: software for one- and two-dimensional real algebraic sets. In *Mathematical software—ICMS 2014*, volume 8592 of *Lecture Notes in Comput. Sci.*, pages 175–182. Springer, Heidelberg, 2014.
- [10] D.A. Brake, J.D. Hauenstein, and C. Vinzant. Bertini_tropical. Available at bertini.nd.edu/tropical.
- [11] J.A. De Loera, B. Sturmfels, and C. Vinzant. The central curve in linear programming. *Found. Comput. Math.*, 12(4):509–540, 2012.
- [12] J.D. Hauenstein, I. Haywood, and A.C. Liddell, Jr. An *a posteriori* certification algorithm for Newton homotopies. In *Proceedings of the 39th International Symposium on Symbolic and Algebraic Computation*, ACM, New York, 2014, pp. 248–255.
- [13] J.D. Hauenstein and A.C. Liddell, Jr. Certified predictor-corrector tracking for Newton homotopies. *Journal of Symbolic Computation*, 74:239–254, 2016.
- [14] J.D. Hauenstein, B. Mourrain, and A. Szanto. Certifying isolated singular points and their multiplicity structure. In *Proceedings of the 40th International Symposium on Symbolic and Algebraic Computation*, ACM, New York, 2015, pp. 213–220.
- [15] J.D. Hauenstein, A.J. Sommese, and C.W. Wampler. Regeneration homotopies for solving systems of polynomials. *Math. Comp.*, 80(273):345–377, 2011.
- [16] J.D. Hauenstein and F. Sottile. Newton polytopes and witness sets. *Math. Comp. Sci.*, 8(2):235–251, 2014.
- [17] J.D. Hauenstein and F. Sottile. Algorithm 921: alphaCertified: certifying solutions to polynomial systems. *ACM Trans. Math. Softw.*, 38(4):28, 2012.
- [18] J.D. Hauenstein and C.W. Wampler. Isosingular sets and deflation. *Found. Comput. Math.*, 13(3):371–403, 2013.
- [19] J.D. Hauenstein and C.W. Wampler. Unification and extension of intersection algorithms in numerical algebraic geometry. Preprint, available at www.nd.edu/~jhauenst/preprints.
- [20] A. Jensen, A. Leykin, and J. Yu. Computing tropical curves via homotopy continuation. *Exp. Math.*, 25(1):83–93, 2016.
- [21] D. Maclagan and B. Sturmfels. *Introduction to tropical geometry*, volume 161 of *Graduate Studies in Mathematics*. American Mathematical Society, Providence, RI, 2015.
- [22] G. Mikhalkin. Enumerative tropical algebraic geometry in \mathbb{R}^2 . *J. Amer. Math. Soc.*, 18(2):313–377, 2005.
- [23] A.P. Morgan, A.J. Sommese, and C.W. Wampler. Computing singular solutions to nonlinear analytic systems. *Numer. Math.*, 58(7):669–684, 1991.

- [24] A.J. Sommese and C.W. Wampler, II. *The Numerical Solution of Systems of Polynomials Arising in Engineering and Science*. World Scientific Publishing Co. Pte. Ltd., Hackensack, NJ, 2005.
- [25] D. Speyer and L. Williams. The tropical totally positive Grassmannian. *J. Algebraic Combin.*, 22(2):189–210, 2005.
- [26] L.F. Tabera. On real tropical bases and real tropical discriminants. *Collect. Math.*, 66(1):77–92, 2015.
- [27] L.N. Trefethen and J.A.C. Weideman. The exponentially convergent trapezoidal rule. *SIAM Review*, 56(3):385–458, 2014.
- [28] C. Vinzant. Real radical initial ideals. *J. Algebra*, 352:392–407, 2012.
- [29] O. Viro. Real plane algebraic curves: constructions with controlled topology. *Algebra i Analiz*, 1(5):1–73, 1989.
- [30] O. Viro. From the sixteenth Hilbert problem to tropical geometry. *Jpn. J. Math.*, 3(2):185–214, 2008.